Urban Forestry & Urban Greening 41 (2019) 127–138

Contents lists available at ScienceDirect

Urban Forestry & Urban Greening

journal homepage: www.elsevier.com/locate/ufug

An integrated study on air mitigation potential of urban vegetation: From a multi-trait approach to modeling

R Baraldi*, C. Chieco, L. Neri, O. Facini, F. Rapparini, L. Morrone, A. Rotondi, G. Carriero

CNR - Institute of Biometeorology, Via P. Gobetti 101, 40129, Bologna, Italy

ARTICLE INFO

Handling Editor: N Nilesh Timilsina

Keywords:
Air pollutant removal
CO_2 storage and sequestration
i-Tree eco
Leaf traits
VOC
Urban greening

ABSTRACT

The ecosystem services provided by urban forests contribute to ameliorate air quality and human well-being in cities. An integrated approach based on direct measurements of leaf functional multi-traits and on estimation of the plant mitigation potential was used for predicting the species-specific impact on air quality of 29 species, including trees and shrubs, commonly present in the urban context. In addition, volatile organic compound (VOC) emissions and ozone forming potential (OFP) of each species were evaluated. At plant levels, pollution deposition equations and the i-Tree Eco model were applied for estimating particulate (PM_{10}) and ozone (O_3) removal potential and for calculating carbon dioxide (CO_2) storage and sequestration by the studied species. The results highlight the plant species-specific ability to capture atmospheric pollutants based on their physiological (CO_2 assimilation and stomatal conductance) and morphological (stomata, trichomes, waxes and cuticular ornamentation) leaf traits. Trees with abundant trichomes, waxes and wrinkled leaf surfaces are considered more suitable for capturing pollutants. Most of the studied species are suitable for urban planning programs as they result for the majority low VOC emitters and consequently are characterized by low or moderate OFP. Annual O_3 and PM_{10} removal of the investigated trees species ranged from about 58–140 g plant^{-1} yr^{-1} and from about 17–139 g plant^{-1} yr^{-1}, respectively. Total tree CO_2 storage ranged from about 164–215 kg plant^{-1} and gross annual CO_2 sequestration from 11 to 20 kg plant^{-1} year^{-1}. *Liriodendron tulipifera*, *Celtis australis*, *Acer campestre* and *Acer platanoides*, were efficient species in capturing PM10 and absorbing O_3. *Prunus cerasifera*, *Quercus cerris*, together with *Celtis australis*, *Acer campestre* and *Acer platanoides*, were efficient for carbon sequestration and storage. As aspected, lower potential of pollutant removal and CO_2 storage and sequestration were estimated for shrubs, due to their smaller leaf area and structure.

1. Introduction

Rising anthropogenic greenhouse gas (GHG) emissions and aerosols are the main drivers of climate change (Kroeger, 2010). Since the beginning of the Industrial Revolution, human activities have produced a relevant increase of GHG such as carbon dioxide (CO_2), nitrogen dioxide (NO_2), methane (CH_4), and ozone (O_3) but also particulate matter (PM), a mixture of heavy metals, black carbon, polycyclic aromatic hydrocarbons and other substances suspended in the atmosphere (Bell et al., 2013). Ozone is the third most important greenhouse gas (Kulkarni et al., 2015) and, together with PM, is the most threatening secondary air pollutants in the cities (EEA, 2017). The European Environment Agency (EEA) estimated that, during 2013 and 2015, the European citizens were exposed to PM_{10} concentrations that were 16–20% and 50–62 % above the EU daily limit values (50 μg m^{-3}) and the annual reference level (20 μg m^{-3}) of the World Health Organization (EEA, 2017). Exposure to O3 have been associated with increased number of hospitalizations and premature mortality for respiratory and cardiovascular diseases (Krmpotic et al., 2015; Nuvolone et al., 2017). Increasing concern surrounding GHG emissions and particles has led to numerous global mitigation efforts (IPCC, 2014; UNFCCC, 2015). A recent study identified and quantified solutions for increasing carbon sequestration and reducing GHG emissions through conservation and improvement of the management practices of forest, wetland and grassland biomes (Griscom et al., 2017). The same study reported that urban greening programs could provide over one third of the cost-effective climate mitigation needed between now and 2030 to stabilize warming to below 2 °C. Forests have long been considered in climate research for their ability to offset emissions by converting CO_2 via photosynthesis in biomass such as leaves, roots, stems and branches (Roy et al., 2012). Vegetation, particularly urban and periurban forests, can consistently reduce pollution levels through dry deposition

* Corresponding author.
E-mail address: baraldi@ibimet.cnr.it (R. Baraldi).

https://doi.org/10.1016/j.ufug.2019.03.020
Received 3 August 2018; Received in revised form 11 February 2019; Accepted 29 March 2019
Available online 30 March 2019
1618-8667/

processes (Manes et al., 2016) thanks to the adsorption of PM on the leaf surface (Sæbø et al., 2012) and the uptake of gaseous pollutants such as O_3 through stomatal flux (Nowak et al., 2006). However plant contribution to urban mitigation depends on complex interactions between biotic and abiotic environmental factors, pollutant concentrations and plant structural and functional characteristics, which can be inferred through parameters such as Leaf Area Index (LAI) and stomatal conductance (g_s) (de Groot et al., 2002).

Leaf structural characteristics (e.g. cuticle, epidermis, epicuticular wax, stomata, and trichomes), together with total leaf area, influence trees and shrubs efficiency in PM removal from urban atmosphere (Wang et al., 2010). Conifers are overall considered to be more effective in PM capture than broadleaved species (Sæbø et al., 2012). Among broadleaved trees, species with rough leaf surfaces are more efficient in PM capturing as surface roughness interacts mainly with fine and ultrafine particles depending on Brownian diffusion (Hwang et al., 2011; EL-Khatib et al., 2011). Epidermal trichomes on leaf surface enable leaves to trap bigger size PM, while ridges and grooves of epidermal cells lining, veins projections and stomata with wax rings enable the trapping of smaller particles (Jamil et al., 2009). Plants, and particularly trees, can release volatile organic compounds (VOC) including isoprenoids (mainly isoprene and monoterpenes) for defense, communication and protection against stress conditions (Loreto et al., 2014). VOC can play a critical role in the biosphere-atmosphere interaction, contributing to the formation or removal of particles and tropospheric ozone, depending on the ratio between VOC and nitrogen oxide (NO_x) concentrations in polluted urban/peri-urban airsheds (Kulmala et al., 2004). Since isoprene and monoterpenes are characterized by different reaction rates with O_3 and NO_x, the chemical speciation of emission is relevant to predict the impact of plant species on air quality (Benjamin and Winer, 1998; Calfapietra et al., 2013). Isoprenoid emission widely differs among tree species and even within species, depending on both physiological and environmental factors (Niinemets et al., 2004; Baraldi et al., 2006). Lists of the tree species most suitable to urban environments are available (Sæbø et al., 2013; Grote et al., 2016), with trees being ranked according to the emitted compounds and their reactivity with oxidizing radicals in the troposphere (Benjamin et al., 1996). Research integrating the cumulative effects of urban vegetation on pollution removal and particularly on carbon sequestration and O_3 formation, is challenging due to the complexity of the physical and chemical processes involved in the trees-atmosphere interactions within urban areas (Cherlin et al., 2015). Indeed, the beneficial effect of urban vegetation can be context-dependent due to the high spatial and temporal variability in and among cities. There is a growing attention on the use of models to study the magnitude of air pollution removal by plants, in particular to estimate deposition, interception and dispersal of pollutants by trees (Brack, 2002). The most used model in urban and peri-urban environment is i-Tree Eco, designed and developed by U.S. Department of Agriculture Forest Service and several partner organizations (USDA, 2015). i-Tree Eco is designed to describe the urban forest structure and its potential in pollutant absorption (Nowak et al., 2008) and it has been used in more than 50 cities across the world (Nowak et al., 2008), even if its use is still limited for European cities (Bottalico et al., 2017).

The overall aim of our study was to estimate the contribution of tree and shrubs species to urban air mitigation. The specific objectives of this study were: (1) to examine species-specific leaf functional traits, including gas exchanges and micro-morphological structures, affecting their potential performance in pollutant reduction; (2) to assess species-specific VOC emission capacity and OFP, for evaluating the ecosystem disservices; (3) to estimate at plant level PM_{10} and O_3 removal by applying pollution deposition equations, and (4) to assess CO_2 storage and sequestration provided by the selected plants using the i-Tree Eco model. The study was carried out on 25 broadleaf tree species and on 4 evergreen shrubs, commonly planted in the city of Bologna (Italy) and surrounding areas, with the purpose to provide sustainable solutions for pollutant mitigation in urban areas and thus to support policy-makers in the selection and management of urban greening.

Table 1
Plant species sampled for this study. BDL = broadleaf deciduous large plants; BDS = broadleaf deciduous small plants; BDM = broadleaf deciduous medium plants; SHR = shrubs.

Scientific name	Common name	Family	Habit
Acer campestre L.	Country maple	Aceraceae	BDL
Acer platanoides L.	Norway maple	Aceraceae	BDL
Alnus glutinosa L.	Black alder	Betulaceae	BDL
Carpinus betulus L.	Hornbeam	Betulaceae	BDL
Catalpa bunjei C.A. Mey.	Manchurian catalpa	Bignoniaceae	BDS
Celtis australis L.	European nettle tree	Ulmaceae	BDL
Cercis siliquastrum L.	Judas tree	Fabaceae	BDS
Crataegus monogyna Jacq.	Hawthorn	Rosaceae	BDS
Fraxinus excelsior L.	European ash	Oleaceae	BDM
Fraxinus ornus L.	Flowering ash	Oleaceae	BDM
Gingko biloba L.	Maidenhair tree	Ginkgoaceae	BDL
Koelreuteria paniculata Laxm.	Golden raintree	Sapindacee	BDM
Laurus nobilis L.	Bay laurel	Lauraceae	SHR
Ligustrum japonicum Thunb.	Wax-leaf privet	Oleaceae	SHR
Liquidambar styraciflua L.	American storax	Altingiaceae	BDM
Liriodendron tulipifera L.	Tulip tree	Magnoliaceae	BDL
Malus domestica Borkh.	Apple tree	Rosaceae	BDS
Morus alba L.	White mulberry	Moraceae	BDS
Prunus cerasifera "pissardii" Ehrh.	Cherry plum	Rosaceae	BDS
Parrotia persica C.A. Mey.	Persian ironwood	Hamamelidaceae	BDM
Photinia x fraseri "Red Robin" Dress.	Red robin	Rosaceae	SHR
Quercus cerris L.	Turkey oak	Fagaceae	BDL
Robinia pseudoacacia L.,	Black locust	Fabaceae	BDM
Sambucus nigra L.	Black elder	Caprifoliaceae	BDS
Sophora japonica L.	Japanese pagoda tree	Fabaceae	BDM
Tilia cordata Mill.	Small-leaved lime	Tiliaceae	BDL
Tilia platyphyllos Scop.	Broad leaved lime	Tiliaceae	BDL
Ulmus minor Mill.	Field elm	Ulmaceae	BDL
Viburnum tinus L.	Laurustinus	Caprifoliaceae	SHR

2. Materials and methods

2.1. Plant material

Twenty-nine species were selected for the study, including 4 evergreen shrubs and 25 urban deciduous broadleaf trees (Table 1). The study was carried out on 3-years-old potted plants grown in well-watered universal potting soil in the nursery of the Institute of Biometeorology of the National Research Council (IBIMET-CNR) in Bologna (Italy) under natural conditions of light, temperature and humidity. Three plants for each species were assessed.

2.2. Measurements of physiological and morphological leaf traits

2.2.1. Leaf carbon assimilation and stomatal conductance

Measurements of carbon assimilation (A) and stomatal conductance (g_s) were carried out using a LI-COR 6400 Photosynthesis System (LI-COR Inc., USA) and were determined on three healthy mature leaves of each of the three plants for species under standard conditions of 30 °C and 1000 μmol m^{-2} s^{-1} PPFD, as reported in Baraldi et al. (2018). The physiological responses were monitored between 9 a.m. and 1 pm in June-July.

2.2.2. Leaf VOC emissions and plant OFP estimation

Standardized VOC emission rates were determined by sampling VOC simultaneously to A and gs measurements: the outlet of the LI-COR leaf chamber was connected to steel tubes packed with 200 mg of Tenax GC® and Carbograph (Markes International, Ltd, Llantrisant, UK) linked

Table 2
CO_2 assimilation (A), stomatal conductance (g_s), isoprene and total monoterpenes emission for the studied species. Data are reported as means ± standard error (n = 3). n.d. = not detected. Ozone forming potential (OFP) is referred to daylight hours. Superscript letters in the same column indicate significant differences at $P < 0.05$.

Species name	A μmol CO_2 m^{-2} s^{-1}	g_s mol H_2O m^{-2} s^{-1}	Isoprene μg g dw^{-1} h^{-1}	Monoterpenes μg g dw^{-1} h^{-1}	OFP g $tree^{-1}$ d^{-1}
Acer campestre	14.0 ± 0.5^{a-d}	0.1 ± 0.02^{efg}	n.d.	1.0 ± 0.4^{d}	0
Acer platanoides	12.5 ± 0.9^{b-h}	1.0 ± 0.1^{a}	0.02 ± 0.0^{d}	4.4 ± 0.3^{b}	1
Alnus glutinosa	8.6 ± 1.7^{k-m}	0.1 ± 0.02^{efg}	0.3 ± 0.3^{d}	1.1 ± 0.04^{d}	0
Carpinus betulus	7.2 ± 0.2^{l-q}	0.05 ± 0.01^{g}	n.d.	3.0 ± 1.6^{bc}	1
Catalpa bungei	10.6 ± 1.6^{h-k}	0.3 ± 0.07^{b}	0.2 ± 0.2^{d}	0.3 ± 0.005^{d}	0
Celtis australis	13.0 ± 0.6^{bcd}	0.2 ± 0.01^{d}	0.01 ± 0.004^{d}	7.6 ± 0.3^{a}	2
Cercis siliquastrum	8.0 ± 0.3^{l-p}	0.2 ± 0.02^{def}	11.1 ± 3.5^{bc}	1.6 ± 0.01^{cd}	7
Crataegus monogyna	10.2 ± 2.5^{f-l}	0.3 ± 0.21^{bc}	n.d.	0.4 ± 0.1^{d}	0
Fraxinus excelsior	9.0 ± 0.2^{i-m}	0.06 ± 0.0001^{g}	n.d.	0.9 ± 0.02^{d}	0
Fraxinus ornus	12.6 ± 0.1^{b-h}	0.3 ± 0.0002^{bc}	n.d.	0.03 ± 0.02^{d}	0
Ginkgo biloba	6.8 ± 0.3^{m-p}	0.1 ± 0.01^{fg}	0.6 ± 0.2^{d}	0.1 ± 0.002^{d}	0
Koelreuteria paniculata	4.7 ± 0.6^{q}	0.06 ± 0.01^{g}	0.7 ± 0.2^{d}	0.1 ± 0.001^{d}	0
Liquidambar styraciflua	9.3 ± 1.0^{i-l}	0.06 ± 0.02^{g}	18.9 ± 2.0^{a}	0.4 ± 0.02^{d}	5
Liriodendron tulipifera	10.2 ± 1.2^{e-l}	0.1 ± 0.002^{efg}	4.1 ± 1.2^{cd}	8.4 ± 1.6^{a}	4
Malus domestica	13.2 ± 2.5^{a-g}	0.1 ± 0.01^{efg}	0.07 ± 0.05^{d}	1.6 ± 1.1^{cd}	0
Morus alba	11.6 ± 0.9^{d-i}	0.1 ± 0.03^{dc}	0.6 ± 0.2^{d}	0.7 ± 0.02^{d}	0
Parrotia persica	15.2 ± 1.3^{ab}	0.1 ± 0.02^{efg}	0.6 ± 0.2^{d}	0.5 ± 0.01^{d}	0
Prunus cerasifera	15.5 ± 0.8^{abc}	0.3 ± 0.02^{b}	0.5 ± 0.0^{d}	0.48 ± 0.01^{d}	0
Quercus cerris	12.2 ± 0.3^{b-i}	0.1 ± 0.0001^{efg}	0.1 ± 0.001^{d}	0.3 ± 0.07^{d}	0
Robinia pseudoacacia	8.6 ± 2.2^{k-n}	0.1 ± 0.05^{efg}	16.0 ± 6.9^{ab}	0.5 ± 0.003^{d}	1
Sambucus nigra	5.7 ± 0.4^{opq}	0.05 ± 0.003^{g}	0.1 ± 0.04^{d}	0.9 ± 0.2^{d}	0
Sophora japonica	9.5 ± 1.7^{ikl}	0.2 ± 0.03^{de}	12.3 ± 3.6^{ab}	0.2 ± 0.003^{d}	7
Tilia cordata	11.9 ± 1.2^{c-j}	0.2 ± 0.01^{cde}	n.d.	3.4 ± 0.1^{b}	1
Tilia platyphyllos	11.3 ± 0.9^{ghi}	0.2 ± 0.03^{de}	0.09 ± 0.004^{d}	7.7 ± 1.23^{a}	2
Ulmus minor	15.5 ± 0.8^{a}	0.3 ± 0.04^{b}	0.2 ± 0.05^{d}	0.4 ± 0.03^{d}	0
Laurus nobilis	5.9 ± 0.3^{pq}	0.06 ± 0.005^{g}	0.1 ± 0.05^{d}	0.8 ± 0.1^{d}	0
Ligustrum japonicum	7.8 ± 0.7^{lmn}	0.1 ± 0.01^{fg}	0.1 ± 0.06^{d}	0.1 ± 0.01^{d}	0
Photinia x fraseri	8.0 ± 0.3^{lmn}	0.1 ± 0.001^{fg}	0.1 ± 0.03^{d}	0.49 ± 0.1^{d}	0
Viburnum tinus	6.2 ± 0.5n^{-q}	0.07 ± 0.001^{g}	0.05 ± 0.02^{d}	1.05 ± 0.2^{d}	0

to an external pump (Pocket Pump SKC Inc., USA). A volume of 2.5 l air was adsorbed at a flow rate of 200 ml min^{-1}, then the samples were processed and analysed with a thermal-desorber (Markes International, Series 2 Unity) connected to a 7890 A gas chromatograph coupled with a 5975C mass detector (GC–MS, Agilent Technologies, Wilmington, USA) as described in Baraldi et al. (2018). Identification and quantification of the sampled isoprenoid iwere carried out according to Rapparini et al. (2004).

OFP was estimated for each species according to Benjamin and Winer (1998) as:

$$OFP = B\ [(E_{iso}R_{iso}) + (E_{mono}R_{mono})],$$

where B is the biomass factor [(g leaf dry weight) $plant^{-1}$], E_{iso} and E_{mono} are species-specific mass emission rates [(μg VOC) g^{-1} leaf dry weight d^{-1}] for isoprene and monoterpenes, respectively, R_{iso} and R_{mono} are reactivity factors [(g O_3 g^{-1} VOC] based upon the Maximum Incremental Reactivity scale (MIRs) provided by Carter (1994). The biomass factors were estimated according to Benjamin and Winer (1998) and Hallik et al. (2009). A reactivity factor of 9.1 g O_3 (g isoprene)$^{-1}$ for isoprene and an average reactivity factor of 3.8 g O_3 (g monoterpene)$^{-1}$ for monoterpenes were assumed. The O_3 formed may depend on NO_x concentrations, meteorological conditions, and atmospheric reactions. In the present study, it was assumed that NO_x and meteorological conditions were not limiting factors in the O_3 produced.

2.2.3. Leaf micromorphological analysis

Leaf micromorphological analyses were carried out with a scanning electron microscope (SEM, LEO 1530; Zeiss, Oberkochen, Germany), as reported in Baraldi et al. (2018), using a glass desiccator to best preserve the wax structure on both surfaces (Chieco et al., 2012). The stomatal density was determined using an image analysis software (Leica Application Suite V4, Germany), taking three images for each sample. Nine total values for the abaxial surface of each species were determined and standardized to 1 mm^2 leaf surface. Trichomes were classified considering typology such as glandular (capitate or peltate) or non-glandular (simple or filiform), and distribution (Hardin, 1992). Epicuticular waxes were classified considering abundance, typology and distribution (Barthlott et al., 1998). Finally, the typology of cuticular ornamentations was investigated (EL-Khatib et al., 2011).

2.3. Estimation of PM_{10} and O_3 removal

Two main air pollutants were considered: particulate matter (PM_{10}) and tropospheric ozone. As reported by other Italian studies (Manes et al., 2014; Bottalico et al., 2017), we modeled air pollution removal at leaf level. The meteorological data (air temperature, photosynthetic active radiation, atmospheric pressure and relative humidity), hourly concentration data for O_3 and monthly concentration for PM_{10} (g m^{-2}) of the year 2015 were provided by two monitoring stations of the Regional Agency for Environmental Protection (ARPAE). The i-Tree Eco model was used to estimate leaf area of medium size tree (diameter at breast height, DBH, 30 cm) and shrub (DBH 10 cm) using equations that predict leaf area index (LAI) and canopy cover for open grown deciduous urban trees based on crown parameters (Nowak et al., 2006). The annual PM_{10} deposition was calculated according to Bottalico et al. (2017) as:

$$PM_{10}\ \text{deposition}\ (g\ m^{-2}) = V_d \times C_i \times T_i \times 24 \times 3600 \times 0.5$$

where V_d is dry deposition velocity (m s^{-1}) for PM_{10}, set to an average 0.0064 m s^{-1} according to Lovett (1994); C_i is mean yearly PM_{10} concentration (μg m^{-3}); T_i is number of days $year^{-1}$ (we assumed 183 days of vegetative period for broadleaves deciduous trees and throughout the year for evergreen shrubs); 0.5 is the 50% of resuspension rate of particles back to the atmosphere (Hirabayashi et al., 2012). Stomatal O_3 fluxes (FO_3) were calculated according to the species-specific parameterizations reported in Bottalico et al. (2017) and Manes et al.

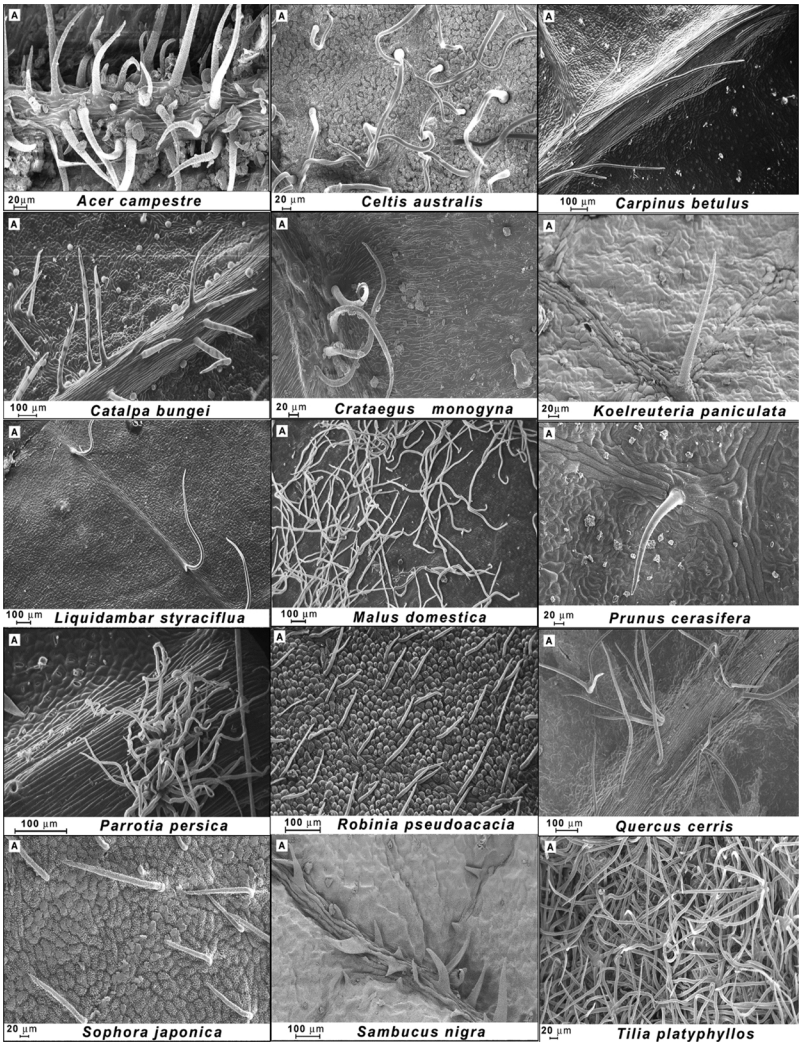

Fig. 1. Scanning electron micrograph of trichomes. A: simple.

(2016):

$$FO_3 = g_{max} \times [O_3] \times 0.613$$

where FO_3 is instantaneous stomatal O_3 flux (nmol m^{-2} s^{-1}); g_{max} is species-specific maximum stomatal conductance to water vapour (mol m^{-2} proiected leaf area s^{-1}) under optimal conditions (Bottalico et al., 2017); $[O_3]$ is O_3 annual concentration in ppb (nmol mol^{-1}); 0.613 is diffusibility ratio between O_3 and water vapor. The instantaneous fluxes were used to calculate the total annual cumulated O_3 fluxes for each species:

$$FO_3 \text{ cum} = FO_3 \times 3600 \times Ph \times 10^{-9}$$

where FO_3 cum is annual cumulated stomatal O_3 flux (mol m^{-2} yr^{-1}); Ph is photoperiod in hours (8 daily hours) and days of the year; 10^{-9} is a dimensional correction factor. It was assumed that stomatal O_3 flux corresponds to 30% of total potential O_3 removal (FO_3 t) consisting of both stomatal and non-stomatal processes: FO_3 t = FO_3cum/0.3. FO_3 t was then converted in g to obtain the annual O_3 absorbed by each species.

2.3.1. CO_2 storage and sequestration

CO_2 storage and sequestration were estimated by the i-Tree Eco Model. This model (formerly Urban Forest Effects – UFORE model) (Nowak et al., 2008) was developed by the U.S. Department of Agriculture Forest Service (Nowak and Crane, 2000; USDA, 2015) and it allows studying the structure and services of the forest ecosystems. Carbon storage and annual sequestration of medium size trees and shrubs were estimated using biomass and allometric equations that combined average values of stem diameter (DBH), tree and crown height, crown width, crown light exposure, and climatic conditions. The allometric equations and conversion factors were taken from the literature to estimate whole tree dry weight biomass (Nowak, 1994; Nowak et al., 2008). To facilitate national estimates of carbon storage and sequestration, the carbon data were standardized per unit of tree cover (Lawrence et al., 2012).

2.3.2. Statistical analysis

Statistical analyses were performed with SAS 9.4/STAT software (SAS Institute, Cary, USA). For the physiological variables, one-way analysis of variance (ANOVA, Newman-Keul test) was used to analyze the differences among treatments. Differences were considered significant with $P < 0.05$.

3. Results and discussion

3.1. Leaf-trait analysis

3.1.1. Results of CO_2 assimilation and stomatal conductance

CO_2 assimilation and stomatal conductance were species-specific as also reported by Gunderson et al. (2002) (Table 2). The highest photosynthesic values were measured in *A. campestre*, *M. domestica*, *P.*

Table 3
Leaf macro and micromorphology of the studied species.

Species	Leaf description	Trichomes	Epicuticular waxes	Cuticular ornamentations
A. campestre	Opposite pairs, broad, with rounded lobes and smooth margin.	Simple trichomes on leaf veins on adaxial surface; capitate trichomes on both leaf surfaces	Absent	Deep ridges and furrows formed by epidermal cell lining and veins projections
A. platanoides	Opposite, palmate with five lobes and smooth margin.	Rare capitate trichomes on abaxial surface	Completely cover on both surfaces	Ridges on both surfaces
A. glutinosa	Obovate, rounded with a slightly wedge-shaped base and a wavy, serrated margin.	Absent	Smooth wax layer on both surfaces	Smooth abaxial surface and ridges formed by epidermal cell lining
C. betulus	Elliptic, ovate and alternate, with prominent veins and a serrated margin.	Simple trichomes on veins on the abaxial surface	Absent	Ridges formed by epidermal cell lining and veins projections on both surfaces
C. bungei	Large and heart shaped.	Simple and capitate trichomes on the abaxial surface	Absent	Ridges and micro-ridges formed by epidermal cell lining and protruding stomata
C. australis	Alternate, narrow and sharp-toothed, wrinkly adaxial and tomentose abaxial surfaces.	Simple trichomes on both abaxial and adaxial surfaces	Wax layer on abaxial surface	Deep micro-ridges on the whole surface and sunken stomata
C. siliquastrum	Cordate with a blunt apex.	Absent	Waxes in platelets covering the whole leaf surfaces	Ridges on the whole leaf surfaces
C. monogyna	Obovate and deeply lobed, spreading at a wide angle with long petiole.	Simple trichomes on both surfaces	Waxes in platelets on the abaxial surface	Major veins raised; stomata unaligned level with surface. Guard cells concave
F. excelsior	Opposite, imparipinnate, with serrated margins	Scarce capitate trichomes on both surfaces	Absent	Striation, converging to stomata; deep ridges, micro ridges and furrows
F. ornus	Opposite imparipinnate; leaflets oblong-ovate with serrated or dentated margin	Peltate trichomes on both surfaces	Smooth waxes on the abaxial surface	Ridges covering the whole surface
G. biloba	Fan-shaped with radiating veins	Absent	Crystalloid rods	Ridges and furrows around the stomata
K. paniculata	Bipinnate with a deeply serrated margin	Simple trichomes on veins on both surfaces. Capitate trichomes on adaxial surface	Waxes in platelets	Ridges and furrows, veins projections converging to stomata on both surfaces
L. styraciflua	Palmate lobed; glabrous, with an entire margin	Few trichomes on veins	Absent	Major vein raised; surface coarsely undulated with deep ridges and furrows
L. tulipifera	Opposite, thick and glabrous, with an entire margin	Absent	Waxes in platelets on the whole surfaces	Major veins raised; extrusions due to the cells dome shape
M. domestica	Elliptic, ovate with serrate margin and with five sharply palmate lobes	Dense simple trichomes on both surfaces	Absent	Protruding stomata and ridges converging to stomata
M. alba	Alternate with four lobes, venation pinnate-reticulate; major veins raised	Simple trichomes on the abaxial surface; glandular capitate trichomes on the adaxial surface	Absent	Ridges and micro-ridges on both leaf surfaces
P. persica	Obovate and elliptic cordate at the base, rounded to acuminate at the tip, serrated margins	Bundle simple trichomes on both the leaf surfaces	Waxes in platelets only on the adaxial surface	Ridges on abaxial leaf surface
P. cerasifera	Oblong-obovate, acuminate with serrated margins	Simple trichomes on veins on both surfaces	Absent	Striation in central portion or continuous
Q. cerris	Glabrous, ovate leaves	Bundle simple trichomes on leaf veins on abaxial surface	Waxes in platelets on adaxial surface	Protruding stomata and ridges on surface
R. pseudoacacia	Imparipinnate, leaflets elliptic to ovate, with wavy margins	Simple trichomes on both surfaces	Abundant waxes in platelets on both surfaces	Deep ridges and furrows formed by protruding cell lining
S. nigra	Imparipinnate leaflets ovate to elliptic long, acuminate; margin serrate	Simple trichomes on major veins on both surfaces	Absent	Continuous striation with ridges and micro-ridges
S. japonica	Imparipinnate, leaflets ovate with triangular lobes on each side	Simple trichomes on both surfaces	Waxes in platelets on both surfaces	Deep ridges and furrows with stomata recessed into surface
T. cordata	Cordate, apiculate, margin finely and sharply serrate	Absent	Crystalloid waxes on the abaxial surface; waxes in granules on the adaxial surface	Deep ridges and furrows and major veins raised
T. platyphyllos	Obliquely cordate, pinnate with five to seven leaflets, with a serrated margin	Dense simple trichomes on both surfaces	Absent	Fine striation on both surfaces; smooth adaxial surface
U. minor	Pinnate with lustrous, dark green leaflets.	Capitate trichomes on the abaxial surface; simple trichomes on leaf veins on the adaxial surface	Waxes in granules on the adaxial surface	Deep ridges and furrows, protruding stomata and vein projections
L. nobilis	Evergreen alternately arranged, rounded to triangular-ovate and glabrous	Absent	Scattered waxes in granules and in platelets on both surfaces	Ridges and furrows, protruding stomata and veins projections
L. japonicum	Evergreen simple, large ovate and cordate, with white downy hair on the underside.	Peltate trichomes on both surfaces	Abundant waxes on both surfaces	Ridges and furrows, protruding stomata and irregular waxy deposits on both surfaces
P. x fraseri	Evergreen, coarse and pubescent at juvanile stage, smooth at mature stage.	Absent	Crystalline waxes with irregular granules covering both surfaces	Deep ridges formed by epidermal cell lining on the whole surface
V. tinus	Evergreen, ovate to elliptic, born in opposite pairs with entire margin.	Absent	Waxes in granules and rodlets on both leaf surfaces	Ridges and furrows, protruding stomata and veins projections on both surfaces

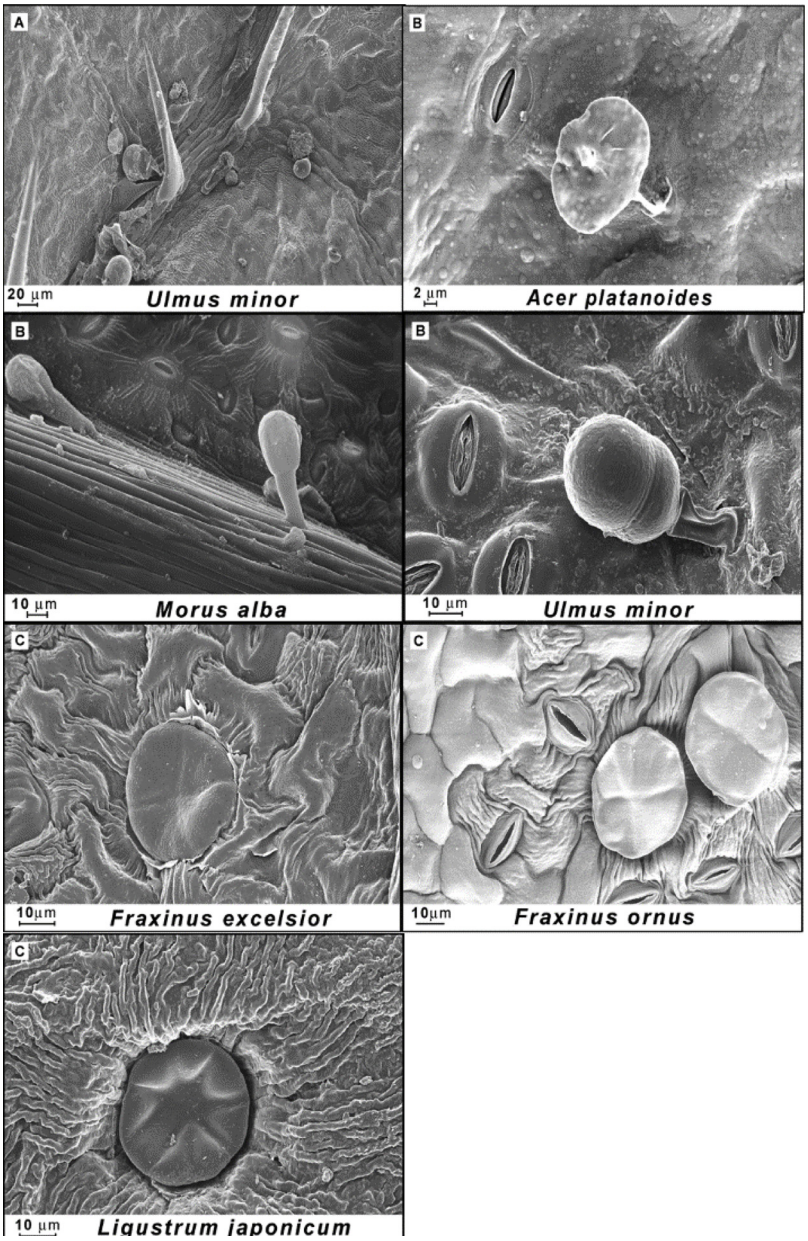

Fig. 2. Scanning electron micrograph of trichomes. A simple, B capitata, C peltata.

cerasifera, *P. persica* and *U. minor* (from 13.2–15.5 µmol CO_2 m^{-2} s^{-1}). The species *A. platanoides, C. bungei, C. australis*, *C. monogyna*, *F.ornus*, *L. tulipifera, M. alba, Q. cerris, T. cordata* and *T. platyphillos* showed medium carbon assimilation rates with values ranging between 10 and 13 µmol CO_2 m^{-2} s^{-1}. The remaining species were characterized by lower photosynthesic rates with values ranging between 9.0 and 4.7 µmol CO_2 m^{-2} s^{-1}. As carbon is a major component of plant structures and is naturally sequestered in plant tissues through photosynthesis, the high CO_2 assimilation, especially in *A. campestre*, *P. cerasifera* and *P. persica*, confirmed the highest CO_2 sequestration from these species (Perlmatter et al., 2017).

Stomatal conductance varied among species, with the highest values found in *A. platanoides* (1.0 mol m^{-2} s^{-1}), followed by C. *bungei, C. monogyna, F. ornus, P. cerasifera, U. minor* with 0.3 mol m^{-2} s^{-1} (Table 2). The tree species *A. campestre, A. glutinosa, C. australis, C. siliquastrum, G. biloba, L. tulipifera, M. domestica, M. alba, P. persica, Q. cerris, R. pseudoacacia, S. japonica, T. cordata, T. plathyphyllos,* and the shrubs *L. japonicum* and *P. fraseri* had medium g_s, with values ranging between 0.20 and 0.10 mol m^{-2} s^{-1}. The remaining species showed the lowest g_s, with values ranging between 0.05 and 0.07 mol m^{-2} s^{-1}. As carbon assimilation is linked to stomatal activity (Singh et al., 2017), the species with the highest gas exchange rates were deemed more suitable for CO_2 mitigation. The differences in gas exchanges across the species illustrate the importance of selecting the most suitable tree and shrub species for urban greening programmes. Stomatal conductance is relevant as it also determines stomatal uptake of air pollutants, and consequently gaseous pollutant reduction (Fowler, 2002). However, pollutants can negatively affect the physiological functions of some plants (Calfapietra et al., 2015). For example it has been reported that O_3 may cause growth reduction in poplar trees (Carriero et al., 2015) and an impairment of physiological traits in deciduous plants (Hoshika et al., 2014) slowing stomatal response to reduced water availability (Paoletti, 2005). Another study reported that NOx exposure induces species-specific changes in growth and phenology, with a consistent trend for accelerated senescence and delayed flowering (Honour et al., 2009). Leaf surface characteristics are also affected by particulate deposition as a long PM exposure may change surface wax structure (Honour et al., 2009). Therefore, the most suitable species for

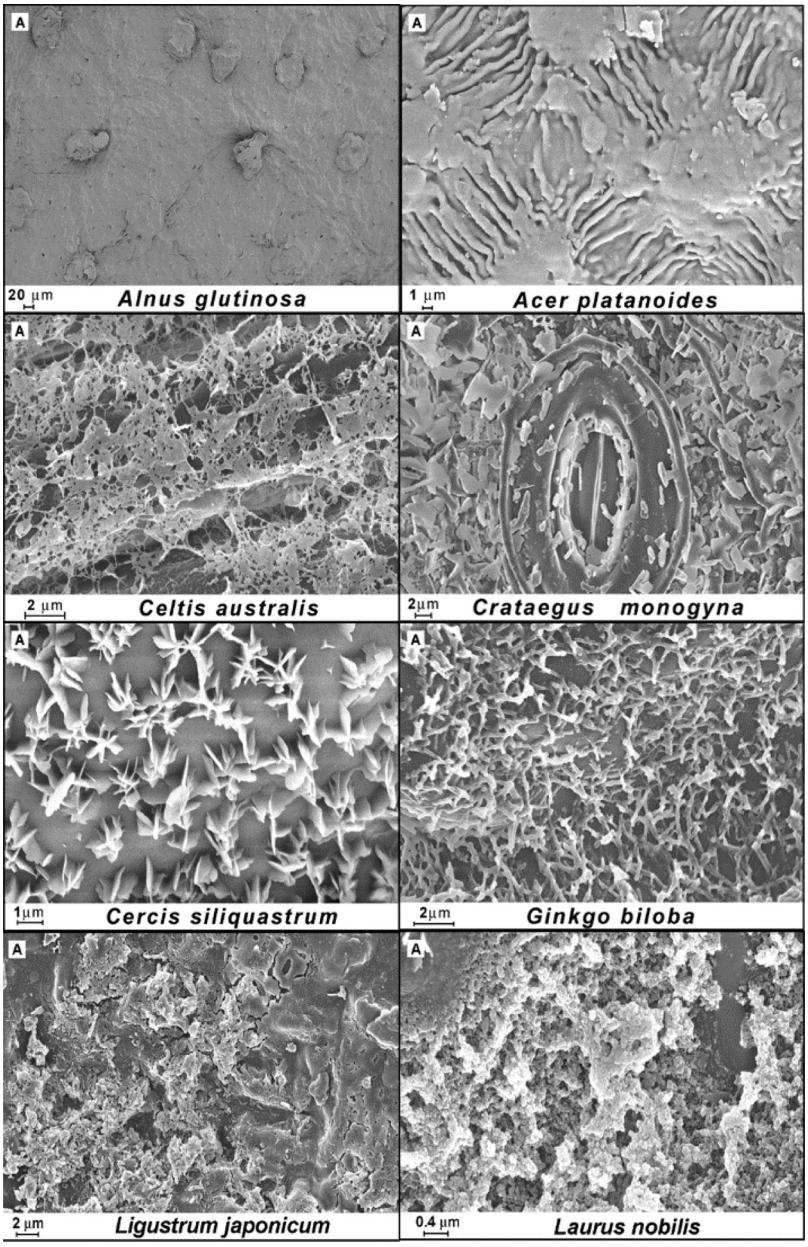

Fig. 3. Scanning electron micrograph of waxes; A Waxes covering the whole leaf surface.

atmospheric pollutants remediation are considered those with the higher stomatal conductance rates and lower pollutants sensitivity (Singh and Verma, 2007).

3.1.2. VOC emission and OFP

VOC emission data reported in Table 2 indicated a species-specific release of isoprenoids, specifically of isoprene and different monoterpenes. Our results on isoprene emitting species are in agreement with previous findings (Benjamin and Winer, 1998; Khedive et al., 2017; Ren et al., 2017; Samson et al., 2017). According to the emission classification by Benjamin et al. (1996) and Wiedinmyer et al. (2004), *L. styraciflua, R. pseudoacacia, S. japonica* and *C. siliquastrum* were identified as high isoprene emitters, *L. tulipifera* as moderate isoprene emitter, while the remaining species were low isoprene emitters. Isoprene emission rate of shrub species resulted negligible.

All the analysed species emitted monoterpenes (Benjamin et al., 1996; Benjamin and Winer, 1998) (Table 2). In particular, moderate monoterpene emission rates were found in *L. tulipifera, T. plathyphyllos, C. australis, A. platanoides*, *T. cordata, C. betulus, C. siliquastrum, M. domestica*, *V. tinus, A. glutinosa* and *A. campestre*, while the remaining species were low emitters. Nineteen monoterpenes were identified by GC–MS analysis: α-pinene, camphene, sabinene, β-pinene, β-myrcene, α-phellandrene, Δ3-carene, α-terpinene, p-cymene, β-phellandrene, 1, 8 cineole, limonene, cis-β-ocimene, trans-β-ocimene, γ-terpinene, α-terpinolene, linalool, camphor. The most representative monoterpenes emitted from all the species were: trans-β-ocimene, representing 23% of the total emitted monoterpenes, sabinene (17%), cis-β-ocimene (14%), β-myrcene (11%), limonene (10%) α-pinene (7%), linalool (3%), β-pinene (3%), and 1, 8 cineol (2%) (data not shown).

The experimental determination of VOC emissions from the selected shrub species showed low emission rates of monoterpenes, with the exception of moderate emissions from *V. tinus,* as previously observed (Benjamin et al., 1996; Shi et al., 2011).

All the species were listed according to their potentiality to form ozone (Benjamin et al., 1996) as species with low OFP, producing less than 1 g O_3 (tree)$^{-1}$ d^{-1}, medium OFP, producing 1–10 g O_3 (tree)$^{-1}$

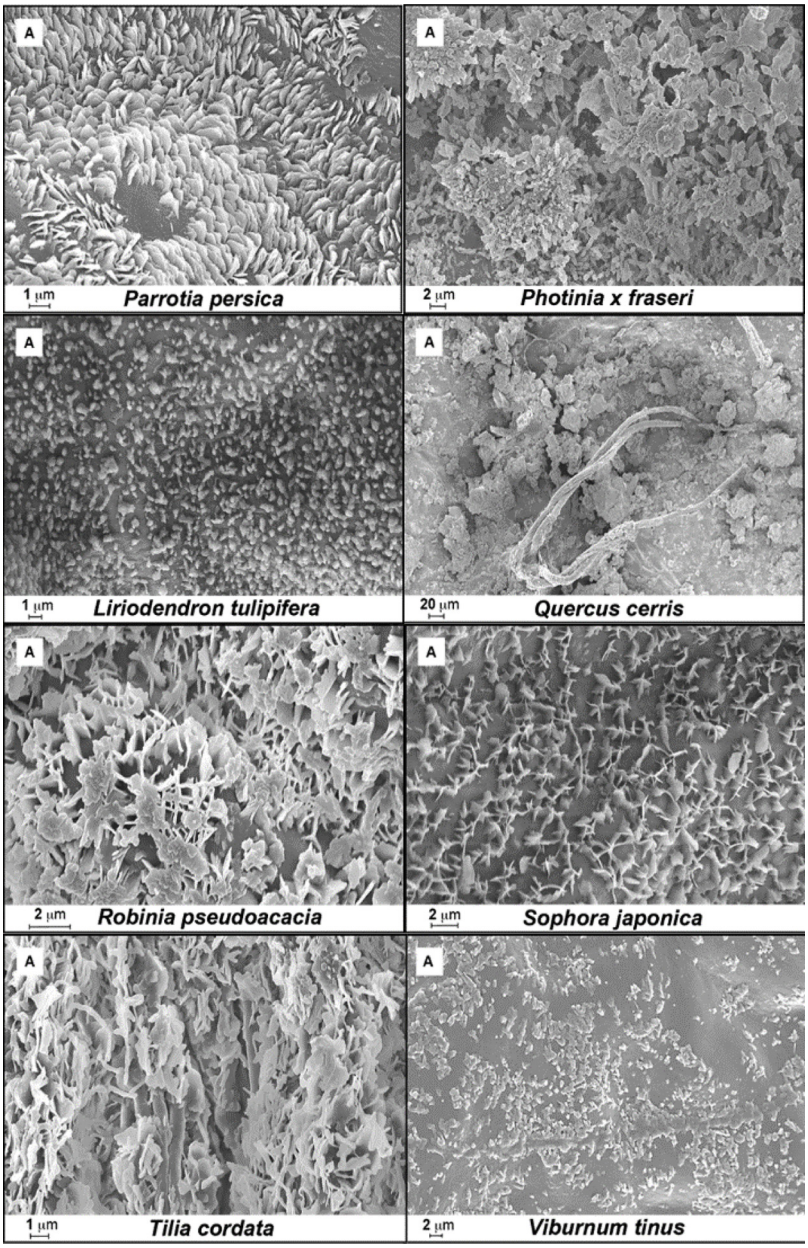

Fig. 4. Scanning electron micrograph of waxes; A Waxes covering the whole leaf surface.

d^{-1}, and high OFP, producing more than 10 g O_3 $(tree)^{-1}$ d^{-1}. Among the studied species, none had high OFP, while *C. siliquastrum, S. japonica*, *L. styraciflua*, *L. tulipifera, C. australis and T. platyphyllos* had medium OFP (Table 2). The remaining species presented low OFP. This OFP variability was due to differences in biomass factors and in the reactivity of the emitted hydrocarbons. Indeed, usually species with high OFP are characterized by high biomass and/or high isoprene emissions whereas species with low OFP have low biomass and/or low isoprene emissions (Benjamin et al., 1998). OFP of a given species, as for the trees and shrubs we studied, is therefore a function not only of the biomass emissions but also of its hydrocarbon speciation profile and the reactivities of the emitted VOC, as well as of locations and emission time (Calfapietra et al., 2013). Emission of volatile isoprenoids is a metabolic cost for plants, but benefits such as improved thermotolerance and higher antioxidant capacity, may outweigh the cost (Fineschi and Loreto, 2012; Loreto and Schnitzler, 2010); it might thus be expected that in a world where temperature and oxidative stress are constantly increasing, BVOC emission from species set in urban environment might vary as well.

3.2. Species-specific leaf morphological traits

3.2.1. Stomata density

Stomata were mostly present on the abaxial surface. The highest stomata density was found in *Q. cerris*, *K. paniculata*, *M. alba*, *A. campestre, L. styraciflua*, *P. persica, C. australis, M. domestica, P. cerasifera,* and *U. minor*, ranging between 400 and 600 stomata mm^{-2}; *F. ornus*, *L. japonicum*, *F. excelsior*, *L. nobilis*, *A. platanoides*, *P. fraseri*, *C. betulus*, *A. glutinosa* and *C. bungei* had a medium stomatal density (between 300 and 200 stomata mm^{-2}) and finally, *C. siliquastrum*, *C. monogyna*, *R. pseudoacacia*, *T. cordata, T. platyphyllos, V. tinus, S. nigra, G. biloba, L. tulipifera,* and *S. japonica* had a low stomata density (between 100 and 200 stomata mm^{-2}) (data not shown). Dust-retention increases with the increase of stomata number (Liu et al., 2012), thus species with higher stomata density are supposed to have the potential to absorb particulate more efficiently.

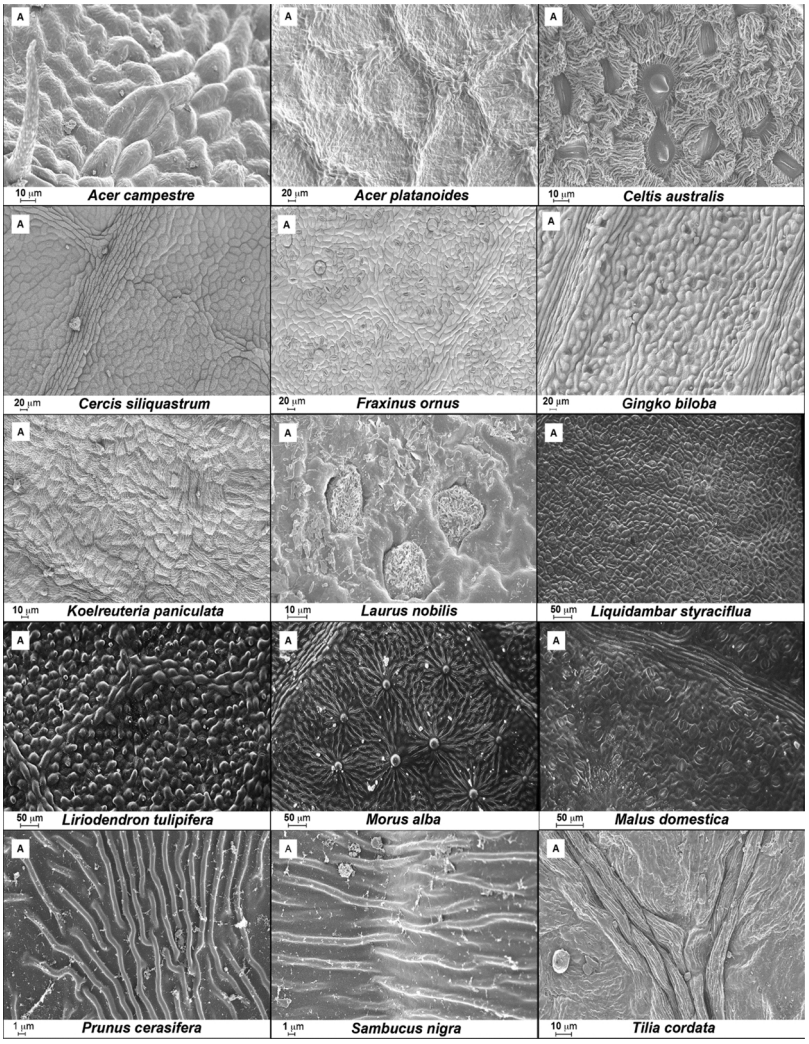

Fig. 5. Scanning electron micrograph of cuticular ornamentations; A ridges and furrows.

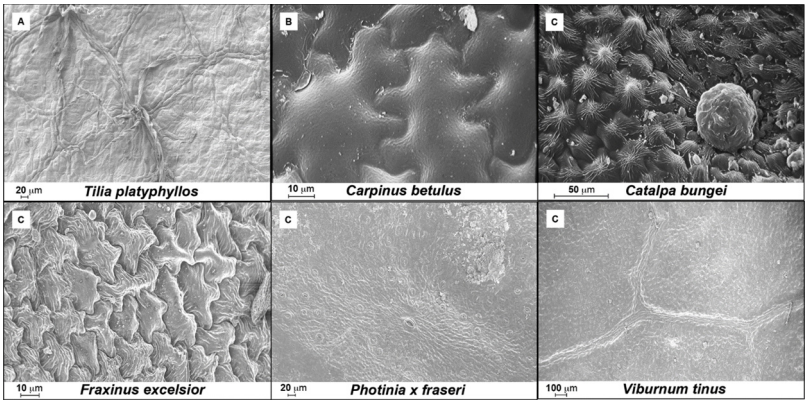

Fig. 6. Scanning electron micrograph of cuticular ornamentations; A fine striation, B ridges and furrows formed by epidermal cells linings, C micro ridges.

3.2.2. Trichomes, waxes and cuticle ornamentations

Trichomes were observed on both the adaxial and the abaxial leaf surfaces of most of the tree species (Fig. 1), with the exception of *A. platanoides C. betulus, C. bungei* and *Q. cerris*, in which trichomes were present only on the abaxial surface and *A. glutinosa*, *C. siliquastrum, G. biloba, L. tulipifera* and *T. cordata*, in which thricomes were completely absent (Table 3). The presence of trichomes on both the leaf surfaces enabled the leaves to trap bigger size particles (Jamil et al., 2009). The shrubs species did not present trichomes, with the exception of *L. japonicum,* characterized by peltate trichomes on both leaf surfaces (Fig. 2). Waxes were present in several tree species, usually as scattered platelets or granules, often completely covering the leaf surface (e.g. C. siliquastrum, *T. cordata*, Figs. 3 and 4). All the shrubs species were characterized by abundant waxes on both abaxial and adaxial leaf surfaces (e.g. *L. Japonicum*, Fig. 3). Leaf surface of both trees and shrub species usually presented ridges, varying in depth, and furrows, formed by epidermal cells linings, protruding stomata or veins projections (e.g. *L. tulipifera*, *M. alba*, Fig. 5); micro ridges were often present as well

Table 4
PM_{10} removal (g plant^{-1} yr^{-1}), O_3 absorption (g plant^{-1} yr^{-1}), carbon storage (kg plant^{-1}) and carbon sequestration (kg plant^{-1}yr^{-1}) of the studied species. Carbon storage and sequestration are calculated with i-Tree Eco model for medium size trees and shrubs.

Species	PM_{10} removal [g plant^{-1} yr^{-1}]	O_3 absorption [g plant^{-1} yr^{-1}]	CO_2 storage [kg plant^{-1}]	Gross CO_2 sequestration [kg plant^{-1} yr^{-1}]
Acer campestre	104.40	137.03	772.63	65.15
Acer platanoides	104.40	137.03	738.59	62.95
Alnus glutinosa	67.82	118.23	703.45	64.78
Carpinus betulus	68.62	140.25	674.17	62.95
Catalpa bungei	44.98	121.20	687.35	63.68
Celtis australis	132.07	133.81	690.28	64.05
Cercis siliquastrum	67.82	118.23	695.03	64.42
Crataegus monogyna	20.85	58.87	662.09	62.22
Fraxinus excelsior	90.34	130.60	637.57	53.80
Fraxinus ornus	76.02	130.60	637.57	53.80
Ginkgo biloba	63.50	109.33	698.32	64.42
Koelreuteria paniculata	72.82	137.03	697.60	64.42
Liquidambar styraciflua	71.50	95.23	602.80	43.55
Liriodendron tulipifera	139.70	127.38	559.61	51.97
Malus domestica	42.14	97.95	655.14	61.49
Morus alba	66.11	115.26	679.30	63.32
Parrotia persica	74.91	92.51	715.90	65.88
Prunus cerasifera	63.63	109.33	789.10	74.66
Quercus cerris	66.12	124.42	784.70	74.66
Robinia pseudoacacia	70.00	115.26	708.21	65.15
Sambucus nigra	17.02	50.46	644.89	60.76
Sophora japonica	49.86	118.23	695.03	64.42
Tilia platyphyllos	71.05	97.95	446.52	40.63
Tilia cordata	72.94	110.32	446.52	40.63
Ulmus minor	94.74	130.60	568.03	52.70
Laurus nobilis	18.82	70.45	54.17	14.27
Ligustrum japonicum	21.16	66.90	56.36	14.27
Photinia x fraseri	18.82	70.45	54.90	13.90
Viburnum tinus	13.58	60.39	49.41	13.54

(e.g. *C. bungei, F. excelsior*, Fig. 6). All the tested species were overall characterized by rough leaf surface, together with abundant trichomes (*A. campestre*, *C. australis*, *M. domestica* and *T. platyphyllos*) or abundant waxes on both leaf surfaces (*A. glutinosa*, *C. siliquastrum, C. monogina*, *F. ornus*, *G. biloba*, *K. paniculata*, *L. tulipifera*, *R. pseudoacacia*, *S. japonica*, *T. cordata*, *L. japonicum*, *and V. tinus*). These morphological characteristics could play a key role in urban mitigation. In fact, pollutant removal ability depends on the presence of trichomes (Liang et al., 2016) and epicuticular waxes (Perini et al., 2017) that trap particles from the atmosphere. Additionally, complex and rough leaf surfaces are more efficient in PM capturing than smooth leaf surfaces (Beckett et al., 2000). In fact micro-roughness such as trichomes, ridges and furrows formed by epidermal cell lining, veins projections, stomata protected with wax rings, cuticular arches, sunken stomata (EL-Khatib et al., 2011), and micro-ridges formed by epidermal projections (Jamil et al., 2009) enhance the capturing of fine and ultrafine particles.

3.3. Plant performance in pollution removal

Leaf structure significantly affects the ability of plants to capture PM (Zhang et al., 2018). Among the studied species, the highest PM10 removal was found in L. tulipifera, *C. australis*, *A. campestre*, *A. platanoides*, *U. minor* and *F. excelsior*, with values ranging from 90 to almost 140 g plant^{-1}yr^{-1} (Table 4). It was assumed that the difference in particle removal among broadleaf trees was due to leaf surface roughness (Hwang et al., 2011). Although the leaf micro- and macro-morphological characteristics of these species (i.e. trichomes, waxes and ridges) were suitable for removing particulate from the urban atmosphere, their high PM_{10} removal was mainly due to the larger leaf area compared to the others (Wang et al., 2010). The values we obtained were in accordance with previous reports, for the species that had already been investigated, such as *L. styraciflua* and *T. cordata* (Grote et al., 2016)

The highest O_3 absorption was found in *C. betulus*, *A. campestre, A. platanoides, K. paniculata, C. australis, F. excelsior, F. ornus and U. minor* with values higher or equal to 130 g plant^{-1}yr^{-1} (Table 4). O_3 uptake depends on stomatal conductance, leaf surface, leaf physiological age, leaf diffusion resistance (Mikkelsen et al., 2004), trunks, leaf cuticular layer and soil moisture (De Santis et al., 2004), that overall contribute to O_3 deposition. In fact, also for the tested species, the O_3 absorption efficiency was mainly affected by both Gs and LAI. The ability of urban forests in removing troposheric O_3 was already demonstrated by Manes et al. (2012), reporting that the large deciduous forest dominated by *Quercus cerris*, characterized in our work by a medium O_3 absorption (around 120 g plant^{-1}yr^{-1}) in Castelporziano, enhanced urban air quality, in a manner related to the physiology and phenology of the species present.

3.4. CO_2 storage and sequestration

The highest CO_2 storage and sequestration was found for *A. campestre, A. platanoides,* C. australis, F. ornus, M. domestica, *P. cerasifera, P. persica*, *Q. cerris* and *U. minor,* while the lowest was found, as aspected, for shrubs (Table 4). Trees act as a sink for CO_2 by fixing carbon during photosynthesis and storing excess carbon as biomass. In fact, the CO_2 storage and sequestration of the species listed above correlated with their photosynthetic efficiency (Table 2). Anyway, larger trees tend to extract and store more CO_2 from the atmosphere, having a greater leaf area (Brack, 2002). Evergreen species, such as shrubs, although having lower CO_2 storage and sequestration abilities than deciduous trees, may contribute to reduce CO_2 throughout the year by their continuous photosynthetic activity, in particular during wintertime, when traffic is more intense (Nowak et al., 2006). Increasing the number of trees in polluted environments could potentially slow the accumulation of CO_2 in the atmosphere.

4. Conclusions

The present study, based on both empirical experiments and modeling studies of plant capacity of air mitigation, supports the evidence of the role played by urban deciduous broadleaves and evergreen species on CO_2 emission offset and pollutants reduction. The multi-trait analysis revealed the importance of interspecific variability in plant features, which have significant functional impacts for pollutant mitigation. The majority of the studied species were characterized by leaf traits enabling plants to effectively trap particles, reduce gaseous pollutants such as O_3 and sequestered CO_2 at the whole plant level, although with different efficiency also affected by leaf areas. Besides, the low or moderate OFP make them suitable for selection of efficient air-mitigating vegetation by urban planting programs aiming at improving urban air quality, according to the environmental benefit to be reached. *Liriodendron tulipifera*, *Celtis australis*, *Acer campestre* and *Acer platanoides*, represent efficient species in capturing PM10 and absorbing O_3. *Prunus cerasifera*, *Quercus cerris*, together with *Celtis australis*, *Acer campestre* and *Acer platanoides*, are suitable for efficiently sequester and storage CO_2. Althought shrubs, for their structural characteristics, are less efficient in pollutant removal and carbon sequestration, their contribution to improving air quality and human health can be relevant, acting as a barrier in the lower strata of planting. Species-specific information is also important to improve model and equations, which do not take into account important plant features and environmental constrains that can enhance or limit the plant potential of pollutant uptake, especially in the Mediterranean region, considered one of

the areas most sensitive to global warming and future climate extreme conditions.H

Mapping the efficieowever, the results of this study.

Acknowledgements

This study was financially supported by the Life + European project GAIA (Green Areas Inner-cities Agreement - http://www.lifegaia.eu). Technical assistance was gratefully received by Matteo Mari and Mafalda Govoni of IBIMET Bologna, and Franco Corticelli of Institute of Microelectronic and Microsystems (IMM) Bologna.

References

Baraldi, R., Rapparini, F., Facini, O., Spano, D., Duce, P., 2006. Isoprenoid emissions and physiological activities of Mediterranean macchia vegetation under field conditions. J. Mediterr. Ecol. 6, 3–9.

Baraldi, R., Neri, L., Costa, F., Facini, O., Rapparini, F., Carriero, G., 2018. Ecophysiological and micromorphological characterization of green roof vegetation for urban mitigation. Urban For. Urban Green in press.

Barthlott, W., Neinhuis, C., Cutler, D., Ditsch, F., Meusel, I., Theisen, I., Wilhelmi, H., 1998. Classification and terminology of plant epicuticular waxes. Bot. J. Linn. Soc. 126, 237–260.

Beckett, K.P., Freer-Smith, P.H., Taylor, G., 2000. The capture of particulate pollution by trees at five contrasting urban sites. Int. J. Urban For. 24, 209–230.

Bell, M.L., Zanobetti, A., Dominici, F., 2013. Evidence on vulnerability and susceptibility to health risks associated with short-term exposure to particulate matter: a systematic review and meta-analysis. Am. J. Epidemiol. 178, 865–876.

Benjamin, M.T., Winer, A.M., 1998. Estimating the ozone-forming potential of urban trees and shrubs. Atmos. Environ. 32, 53–68.

Benjamin, M.T., Sudol, M., Bloch, L., 1996. Low-emitting urban forests: a taxonomic methodology for assigning isoprene and monoterpene emission rates. Atmos. Environ. 30, 1437–1452.

Bottalico, F., Travaglini, D., Chirici, G., Garfì, V., Giannetti, F., De Marco, A., Fares, S., Marchetti, M., Nocentini, S., Paoletti, E., Salbitano, F., Sanesi, G., 2017. A spatially explicit method to assess the dry deposition of air pollution by urban forests in the city of Florence, Italy. Urban For. Urban Green. 27, 221–234.

Brack, C.L., 2002. Pollution mitigation and carbon sequestration by an urban forest. Environ. Pollut. 116, S195–S200.

Calfapietra, C., Fares, S., Manes, F., Morani, A., Sgrigna, G., Loreto, F., 2013. Role of Biogenic Volatile Organic Compounds (BVOC) emitted by urban trees on ozone concentrations in cities: a review. Environ. Pollut. 183, 71–80.

Calfapietra, C., Peñuelas, J., Niinemets, Ü., 2015. Urban plant physiology: adaptation-mitigation strategies under permanent stress. Trends Plant Sci. 20, 72–75.

Carriero, G., Emiliani, G., Giovannelli, A., Hoshika, Y., Manning, W.J., Traversi, M.L., Paoletti, E., 2015. Effects of long-termambient ozone exposure on biomass and wood traits in poplar treated with ethylenediurea (EDU). Environ. Pollut. 206, 575–581.

Carter, W.P.L., 1994. Development of ozone reactivity scales for volatile organic compounds. J. Air Waste Manage. Assoc. 44, 881–899.

Cherlin, N., Roustan, Y., Mousson-Genon, L., Seigneur, C., 2015. Modelling atmospheric dry deposition in urban areas using an urban canopy approach. Geosci. Model. Dev. 8, 893–910.

Chieco, C., Rotondi, A., Morrone, L., Rapparini, F., Baraldi, R., 2012. An ethanol-based fixation method for anatomical and micro-morphological characterization of leaves of various tree species. Biotech. Histochem. 88, 109–119.

de Groot, R.S., Wilson, M.A., Boumans, R.M., 2002. A typology for the classification, description, and valuation of ecosystem functions, goods and services. Ecol. Econ. 41, 393–408.

De Santis, F., Zona, D., Bellagotti, R., Vichi, F., Allegrini, I., 2004. Ozone monitoring in a Mediterranean forest using diffusive and continuous sampling. Anal. Bioanal. Chem. 380, 818–823.

EEA, 2017. Exceedance of Air Quality Standards in Urban Areas. European Environment Agency, Luxembourg.

El-Khatib, A.A., El-Rahman, A.M., Elsheikh, O.M., 2011. Leaf geometric design of urban trees: potentiality to capture airborne particle pollutants. J. Environ. Stud. 7, 49–59.

Fineschi, S., Loreto, F., 2012. Leaf volatile isoprenoids: an important defensive armament in forest tree species. Iforest-Biogeosci. For. 5, 13.

Fowler, D., 2002. In: Bell, J.N.B., Treshow, M. (Eds.), Pollutant Deposition and Uptake by Vegetation. Air Pollution and Plant Life, 2nd ed. Wiley, New York, pp. 43–67.

Griscom, H.P., Griscom, B.W., Ashton, M.S., 2017. Forest regeneration from pasture in the dry tropics of Panama: effects of cattle, exotic grass, and forested riparia. Restor. Ecol. 17, 117–126.

Grote, R., Mayrhofer, S., Fischbach, R.J., Steinbrecher, R., Staudt, M., Schnitzler, J.P., 2016. Process-based modelling of isoprenoid emissions from evergreen leaves of *Quercus ilex* L. Atmos. Environ. 40, 152–165.

Gunderson, C.A., Sholtis, J.D., Wullschleger, S.D., Tissue, D.T., Hanson, P.J., Norby, R.J., 2002. Environmental and stomatal control of photosynthetic enhancement in the canopy of a sweetgum (*Liquidambar styraciflua* L.) plantation during 3 years of CO_2 Enrichment. Plant Cell Environ. 25, 379–393.

Hallik, L., Niinemets, Ü., Wright, I.J., 2009. Are species shade and drought tolerance reflected in leaf-level structural and functional differentiation in northern hemisphere temperate woody flora? New Phytol. 184, 257–274.

Hardin, J.H., 1992. Foliar Morphology of the Common Trees of North Carolina and Adjacent States. North Carolina Agricultural Research Service Technical Bulletin, 298.

Hirabayashi, S., Kroll, C.N., Nowak, D.J., 2012. Development of a distributed air pollutant dry deposition modeling framework. Environ. Pollut. 171, 9–17.

Honour, S.L., Bell, J.B., Ashenden, T.W., Cape, J.N., Power, S.A., 2009. Responses of herbaceous plants to urban air pollution: effects on growth, phenology and leaf surface characteristics. Environ. Pollut. 157, 1279–1286.

Hoshika, Y., Carriero, G., Feng, Z., Zhang, Y., Paoletti, E., 2014. Determinants of stomatal sluggishness in ozone-exposed deciduous tree species. Sci. Total Environ. 481, 453–458.

Hwang, H.J., Yook, S.J., Ahn, K.H., 2011. Experimental investigation of submicron and ultrafine soot particle removal by tree leaves. Atmos. Environ. 45, 6987–6994.

IPCC, 2014. Intergovernmental panel on climate change. Climate Change 2014: Impacts, Adaptation, and Vulnerability. Accessed March 2018. http://www.ipcc.ch/report/ar5/wg2/.

Jamil, S., Abhilash, P.C., Singh, A., Singh, N., Behl, H.M., 2009. Fly ash trapping and metal accumulating capacity of plants: implication for green belt around thermal power plants. Landsc. Urban Plan. 92, 136–147.

Khedive, E., Shirvany, A., Assareh, M.A., Sharkey, T.D., 2017. In situ emission of BVOCs by three urban woody species. Urban For. Urban Green. 21, 153–157.

Krmpotic, D., Luzar-Stiffler, V., Herzog, P., 2015. Effects of urban ozone pollution on hospitalizations for exacerbation of chronic obstructive pulmonary disease. Eur. Respir. J. 46, PA3411.

Kroeger, T., 2010. Black carbon emissions in Asia: sources, impacts and abatement opportunities. Contractor Report Prepared by International Resources Group for USAID, ECO-Asia Clean Development and Climate Program. USAID Regional Development Mission for Asia, Bangkok, Thailand.

Kulkarni, P.S., Bortoli, D., Domingues, A., Silva, A.M., 2015. Surface ozone variability and trend over urban and suburban sites in Portugal. Aerosol Air Qual. Res. 16, 138–152.

Kulmala, M., Vehkamäki, H., Petäjaä, T., Dal Maso, M., Lauri, A., Kerminen, V.M., Birmili, W., McMurry, P.H., 2004. Formation and growth rate of ultrafine atmospheric particles: a review of observations. J. Aerosol Sci. 35, 143–176.

Lawrence, A., De Vreese, R., Johnston, M., van den Bosch, C.C.K., Sanese, G., 2012. Urban forest governance: towards a framework for comparing approaches. Urban For. Urban Green. 12 646-473.

Liang, D., Ma, C., Wang, Y., qi, Wang, Y., jie, Chen-xi, Z., 2016. Quantifying $PM_{2.5}$ capture capability of greening trees based on leaf factors analysing. Environ. Sci. Pollut. Res. - Int. 23, 21176–21186.

Liu, L., Guan, D., Peart, M.R., 2012. The morphological structure of leaves and the dust-retaining capability of afforested plants in urban Guangzhou, South China. Environ. Sci. Pollut. Res. - Int. 19, 3440–3449.

Loreto, F., Schnitzler, J.P., 2010. Abiotic stresses and induced BVOCs. Trends Plant Sci. 15, 154–166.

Loreto, F., Dicke, M., Schnitzler, J.P., Turlings, C.J., 2014. Plant volatiles and the environment. Plant Cell Environ. 37, 1905–1908.

Lovett, G.M., 1994. Atmospheric deposition of nutrients and pollutants in North America: an ecological perspective. Ecol. Appl. 4, 629–650.

Manes, F., Incerti, G., Salvatori, E., Vitale, M., Ricotta, C., Costanza, R., 2012. Urban ecosystem services: tree diversity and stability of tropospheric ozone removal. Ecol. Appl. 22, 349–360.

Manes, F., Silli, V., Salvatori, E., Incerti, G., Galante, G., Fusaro, L., Perrino, C., 2014. Urban ecosystem services: tree diversity and stability of PM10 removal in the metropolitan area of Rome. Ann. Bot. 4, 19–26.

Manes, F., Marando, F., Capotorti, G., Blasi, C., Salvatori, E., Fusaro, L., Ciancarella, L., Mircea, M., Marchetti, M., Chirici, G., Munafò, M., 2016. Regulating ecosystem services of forests in ten Italian metropolitan cities: air quality improvement of PM_{10} and O_3 removal. Ecol. Indic. 67, 425–440.

Mikkelsen, T.N., Ro-Poulsen, H., Hovmand, M.F., Jensen, N.O., Pilegaard, K., Egeløv, A.H., 2004. Atmos. Environ. 38, 2361–2371.

Niinemets, Ü., Loreto, F., Reichstein, M., 2004. Physiological and physicochemical controls on foliar volatile organi compound emissions. Trends Plants Sci. 9, 180–186.

Nowak, D.J., Crane, D.E., Stevens, J.C., 2006. Air pollution removal by urban trees and shrubs in the United States. Urban For. Urban Green. 4, 115–123.

Nowak, D.J., Crane, D.E., Stevens, J.C., Hoehn, R.E., Walton, J.T., 2008. A ground-based method of assessing urban forest structure and ecosystem services. Arboric. Urban For. 34, 347–358.

Nuvolone, D., Petri, D., Voller, F., 2017. The effects of ozone on human health. Environ. Sci. Pollut. Res. - Int. 25, 8074–8088.

Paoletti, E., 2005. Ozone slows stomatal response to light and leaf wounding in a Mediterranean evergreen broadleaf, Arbutus unedo. Environ. Pollut. 134, 439–445.

Perini, K., Ottelè, M., Giulini, S., Magliocco, A., Roccotiello, E., 2017. Quantification of fine dust deposition on different plant species in a vertical greening system. Ecol. Eng. 100, 268–276.

Perlmatter, D., Calfapietra, C., Samson, R., O' Brien, L., Ostoić, S.K., Sanesi, G., Alonso, R., 2017. The Urban Forests- Cultivating Green Infrastructure for People and the Environment, eds. Springer ISBN 978-3-319-50279-3.

Rapparini, F., Baraldi, R., Miglietta, F., Loreto, F., 2004. Isoprenoid emission in trees of *Quercus pubescens* and *Quercus ilex* with lifetime exposure to naturally high CO_2 environment. Plant Cell Environ. 27, 381–391.

Ren, Y., Qu, Z., Du, Y., Xu, R., Ma, D., Yang, G., Shi, Y., Fan, X., Tani, A., Guo, P., Ge, Y., Chang, J., 2017. Air quality and health effects of biogenic volatile organic compounds emissions from urban green spaces and the mitigation strategies. Environ. Pollut. 230, 849–861.

Roy, S., Byrne, J., Pickering, C., 2012. A systematic quantitative review of urban tree

benefits, costs and assessment methods across cities in different climatic zones. Urban Urban Green. 11, 351–363.
Sæbø, A., Popek, R., Nawrot, B., Hanslin, H.M., Gawronska, H., Gawronski, S.W., 2012. Plant species differences in particulate matter accumulation on leaf surfaces. Sci. Total Environ. 427, 347–354.
Sæbø, A., Hanslin, H.M., Baraldi, R., Rapparini, F., Gawronska, H., Gawronski, S.W., 2013. Characterization of urban trees and shrubs for particulate deposition, carbon sequestration and BVOC emissions. Acta Hortic. 990, 509–516.
Samson, R., Grote, R., Calfapietra, C., Cariñanos, P., Fares, S., Paoletti, E., Tiwary, A., 2017. Urban trees and their relation to air pollution. Urban For. Urban Green. 7, 21–30.
Shi, H., Wang, H.X., Li, Y., Liu, X., 2011. Leaf surface microstructure of *Ligustrum lucidum* and *Viburnum odoratissimum* observed by atomic force microscopy (AFM). Acta Ecol. Sin. 31, 1471–1477.
Singh, S.N., Verma, A., 2007. Phytoremediation of air pollutants: a review. Environ. Bioremediat. Technol. 293–314.
Singh, H., Savita, Sharma, R., Sinha, S., Kumar, M., Kumar, P., Verma, A., Sharma, S.K., 2017. Physiological functioning of *Lagerstroemia speciosa* L. under heavy roadside traffic: an approach to screen potential species for abatement of urban air pollution. Biotechnology 61, 1–10.
UNFCCC, 2015. United Nations framework convention on climate change, Paris. COP 21 Climate Agreement. Available at. unfccc.int/resource/docs/2015/cop21/eng/l09r01.pdf.
USDA, 2015. I-Tree Eco Manual. Northern Research Station. USDA Forest Service. https://www.itreetools.org/resources/manuals/Eco_Manual_v5.pdf.
Wang, H.X., Shi, H., Li, Y.Y., 2010. Relationships between leaf surface characteristics and dust-capturing capability of urban greening plant species. Chin. J. Appl. Ecol. 21, 3077–3082.
Wiedinmyer, C., Guenther, A., Harley, P., Hewitt, N., Geron, C., Artaxo, P., Steinbrecher, R., 2004. Global organic emissions from vegetation. Emiss. Atmos. Trace Compd. 18, 115–170.
Zhang, W., Zhang, Z., Meng, H., Zhang, T., 2018. How does leaf surface micromorphology of different trees impact their ability to capture particulate matter? Forests 9, 681–691.